Threshold resummation for Z-boson pair production at NNLO+NNLL

Pulak Banerjee, a,b Chinmoy Dey, a M. C. Kumar a and Vaibhav Pandey a

^aDepartment of Physics, Indian Institute of Technology Guwahati, Guwahati-781039, India

E-mail: pulak.banerjee@lnf.infn.it, d.chinmoy@iitg.ac.in, mckumar@iitg.ac.in, vphiitg@iitg.ac.in

Abstract: The production of a pair of on-shell Z-bosons is an important process at the Large Hadron Collider. Owing to its large production cross section at the LHC, this process is very useful for SM precision studies, electroweak symmetry breaking sector as well as to unravel the possible new physics. In this work, we have performed the threshold resummation of the large logarithms that arise in the partonic threshold limit $z \to 1$, up to Next-to-Next-to-Leading Logarithmic (NNLL) accuracy. The presence of the two-loop contributions in the process dependent resummation coefficient g_0 makes the numerical computation a non-trivial task. After matching the resummed predictions to the Next-to-Next-to-Leading order (NNLO) fixed order results, we present the invariant mass distribution to NNLO+NNLL accuracy in QCD for the current LHC energies. We find that in the high invariant mass region (Q = 1 TeV), while the NNLO corrections are as large as 83% with respect to the leading order, the NNLL contribution enhances the cross section by additional few percent, about 4% for 13.6 TeV LHC. In this invariant mass region, the conventional scale uncertainties in the fixed order results get reduced from 3.4% at NNLO to about 2.6% at NNLO+NNLL, and this reduction is expected to be more for higher Q values.

Keywords: Resummation, perturbative QCD, LHC

^bIstituto Nazionale di Fisica Nucleare, Gruppo collegato di Cosenza, I-87036 Arcavacata di Rende, Cosenza, Italy

Co	ontents	
1	Introduction	1
2	Theoretical Framework	3
3	Numerical Results	6
4	Conclusions	12
A	Resummation coefficients	14

1 Introduction

The production of a pair of massive gauge bosons (Z) at the Large Hadron Collider (LHC) is an important process which has been studied very well both theoretically and experimentally. This process offers very clean signals that can be used to test the prediction of the Standard Model (SM) precisely, thanks to their moderately large production cross sections at the current LHC energies. The process can also be used for testing the SM electroweak symmetry breaking mechanism as well as in the study of fundamental weak interactions among elementary particles. Owing to the large coupling between the Higgs and massive gauge bosons, the process plays an important role in the Higgs sector. One of the important decay modes of Higgs being to a pair of massive gauge bosons, either ZZ or WW.

The experimental signature of this process typically involves either four charged leptons, two leptons plus missing energy or two leptons plus two jets or four jet events. Out of these, the decay to four charged leptons provides a very clean signal in the collider experiments, that led to the measurement of these final states both at the ATLAS and CMS experiments for different centre of mass energies e.g. 5.02 TeV [1], 7 TeV [2–5], 8 TeV [5–10], 13 TeV [10–15] and 13.6 TeV [16]. Such measurements can be used to probe the trilinear gauge couplings as well as to probe the possible hidden new physics. From the theoretical point of view, a similar study can easily be extended to the production of a pair of new massive gauge bosons.

Owing to the importance of this process, a precise knowledge of this process, specifically their production cross sections as well as various kinematic distributions at the current LHC and future high energetic hadron colliders, is very important. In the perturbative Quantum Chromodynamics (pQCD), the leading order (LO) predictions for this process have been available for a long time [17–20]. It is well known that the LO predictions are unreliable and are contaminated with large theoretical uncertainties. The next-to-leading order (NLO) calculations in pQCD were obtained for both on-shell as well as off-shell Z-bosons decaying to a pair of leptons. The NLO QCD corrections for this process can be

found in Ref. [21–23]. The NLO QCD results, matched with Parton Shower (NLO+PS) has been studied in Monte Carlo programmes like POWHEG [24, 25] and aMC@NLO [26]. The ZZ production at the LHC has been analyzed in the context of Beyond Standard Model (BSM) scenarios as well [27]. It is to be noted that at the lowest order in the perturbation theory, this is a quark anti-quark initiated process similar to the Drell-Yan (DY) production of dileptons. However, the Z-boson pair production process has more similarities to the diphoton production process, as both them involve identical particles in the final state, and both are t and u channel processes, whereas DY is a s-channel process (s,t) and u being the Mandelstam variables). For the diphoton production process even at LO, simple kinematic cuts are required to avoid divergences in the forward region, whereas for the case of ZZ production the mass of the Z-boson avoids such divergences, and hence the total production cross section is finite even in absence of any kinematic cuts. However, in the high invariant mass region, or in the region where Z-boson carries much larger kinetic energy compared to the rest mass energy, both the processes can have similar behaviour in the cross sections, the special difference being the isolation algorithm to be used in the case of di-photon production process.

Precision studies entail going beyond NLO. However, for the Z boson pair production process, even the NNLO results are challenging for both analytical as well numerical calculations. The full NNLO calculations have been carried out in [28–30] in QCD for the quark annihilation process. It is also worth noting that the NNLO corrections are computed for both on-shell Z-boson [31, 32] case as well as for off-shell Z-bosons [33, 34] followed by their decay to lepton final states. With the availability of two loop helicity amplitudes [30], the differential distributions for the latter case also became possible. Fiducial cross sections and distributions are also available for the vector boson pair production processes [33, 35]. Additionally, the leading-order process in the gluon fusion channel, $qq \to ZZ$, also contributes at $\mathcal{O}(\alpha_s^2)$. In the low invariant mass region, the gluon fluxes for LHC energies are very large and hence the contribution from this channel near the hadronic threshold region is very crucial and can not be neglected. Going beyond NNLO for ZZ production processes is a challenging task. On the other hand, for DY and Higgs production this has been achieved. Recently the full N³LO results for DY have become available and can be found in Ref. [36–39] and soft-virtual (SV) [40–42] and next-to-soft-virtual (NSV) [43, 44] thershold resummation of DY-type processes are available. The Higgs production through gluon fusion channel N³LO results are available in [45, 46] and SV [47–50] and NSV [43, 51, 52] thershold resummation results are also available. For Higgs production via bottom quark annihilation, SV [53] and NSV [54] resummation results are also available. Rapidity resummation for DY processes are available for SV [55, 56] and NSV [57–60]. Rapidity resummation for gluon fusion channel Higgs production are available for SV [61] and NSV [57, 62] cases. Rapidity resummation for Higgs production via bottom quark annihilation is also available at NNLO+NNLL in Ref. [63]. Nevertheless, for Z-boson pair in the final state, there has been a tremendous effort to go beyond NNLO. Transverse momentum resummation for vector boson pair production is available up to NNLO+N³LL [64, 65]. The parton shower matched with NNLO (NNLO+PS) are recently studied using MINNLO_{PS} [66] method for the ZZ production. The LO matching with parton shower results are available for the gluon fusion channel as well in Ref. [67]. The NLO corrections to this channel have also become available [68–71]. However, their contribution in the high invariant mass region ($\geq 2000~{\rm GeV}$) becomes much smaller than those in the quark annihilation channel. The NLO results matching with parton shower (NLO+PS) results for gluon fusion channel with massless quarks are also available [72]. Finally, at this precision level, the electroweak corrections can not be ignored for precision studies and the NLO EW corrections to this process have been computed in [73–75]. Using SCET formalism, threshold resummation for vector boson pair production is available up to NLO+NNLL [76].

While the threshold resummation for the final state on-shell Z-bosons has been done till NLO+NNLL, it is necessary to go beyond this accuracy. With the increase in experimental precision, it is pertaining to include the effects of higher order effects, particularly at NNLO+NNLL. This manuscript aims to perform the necessary studies that are needed for the precision phenomenology of two on-shell Z-bosons at NNLO+NNLL accuracy. Our paper is organized as follows: We present the theoretical framework in section 2. Details of the phenomenological analysis and the numerical results are presented in section 3. Finally, in section 4, we conclude.

2 Theoretical Framework

The hadronic cross-section for Z-boson pair production can be written in terms of its partonic counterpart as following:

$$\frac{d\sigma}{dQ} = \sum_{a,b=\{q,\bar{q},q\}} \int_0^1 dx_1 \int_0^1 dx_2 \ f_a(x_1,\mu_F^2) f_b(x_2,\mu_F^2) \int_0^1 dz \ \delta\left(z - \frac{\tau}{x_1 x_2}\right) \frac{d\hat{\sigma}_{ab}}{dQ} \ . \tag{2.1}$$

The hadronic and partonic threshold variables τ and z are defined as

$$\tau = \frac{Q^2}{S}, \qquad z = \frac{Q^2}{\hat{s}},$$
(2.2)

where S and \hat{s} are the hadronic and partonic center of mass energies, respectively. τ and z are thus related by $\tau = x_1 x_2 z$.

The leading order Drell-Yan (DY)-type parton level process has the generic form

$$q(p_1) + \bar{q}(p_2) \to Z(p_3) + Z(p_4).$$
 (2.3)

The leading-order (LO) cross-section $\hat{\sigma}_{q\bar{q}}^{(0)}$ for Z-boson pair production can be written as,

$$\frac{d\hat{\sigma}_{q\bar{q}}^{(0)}}{dQ} = \frac{1}{2s} \int dP S_2 \, \mathcal{M}_{(0,0)},\tag{2.4}$$

where dPS_2 is the 2-body phase space integration and $\mathcal{M}_{(0,0)}$ is the born amplitude, which in $d = 4 - 2\epsilon$ dimensions is given below,

$$\mathcal{M}_{(0,0)} = B_f N(c_a^4 + 6c_a^2 c_v^2 + c_v^4) \frac{4}{t^2 u^2} \left\{ -m_z^4 t^2 + 8m_z^4 t u + t^3 u - m_z^4 u^2 + t u^3 - 4m_z^2 t u (t+u) \right\}$$

$$+ \epsilon \left(-2m_z^4 t^2 - 6m_z^4 t u - 2t^3 u + 2m_z^4 u^2 + 2t^2 u^2 - 2t u^3 + 4m_z^2 t u (t+u) \right)$$

$$+ \epsilon^2 \left(-m_z^4 t^2 - 2m_z^4 t u + t^3 u - m_z^4 u^2 + 2t^2 u^2 + t u^3 \right)$$
(2.5)

In Eq. (2.5) the kinematical variables s, t and u are defined as,

$$(p_1 + p_2)^2 = s$$
, $(p_1 - p_3)^2 = t$, $(p_2 - p_3)^2 = u$ and $s + t + u = 2m_z^2$, (2.6)

$$B_f = \frac{(4\pi\alpha)^2}{4N^2} \,, \quad c_v = \frac{\left(T_3^f - 2\sin^2\theta_w Q_f\right)}{2\sin\theta_w \cos\theta_w} \,, \quad c_a = \frac{1}{4\sin\theta_w \cos\theta_w} \,,$$

where the Q_f and T_3^f are the electric charge and third component of weak isospin of the fermion f and θ_w is the weak mixing angle. Here m_z is the mass of Z-boson, N is the SU(N) color, and α is the fine structure constant.

Beyond LO, the partonic cross section receives corrections originating from virtual and real contributions. It is interesting to study the cross-section in the soft limit, which is defined by, $z \to 1$. This means that the initial partonic center of mass energy is almost used to produce the final state pair of Z-bosons, and small energy is left to produce soft partons. In this limit, the partonic cross section can be organized as follows:

$$\frac{d\,\hat{\sigma}_{ab}}{d\,Q} = \frac{d\,\hat{\sigma}_{ab}^{(0)}}{d\,Q} \left(\Delta_{ab}^{\text{sv}}\left(z,\mu_F^2\right) + \Delta_{ab}^{\text{reg}}\left(z,\mu_F^2\right) \right) \,. \tag{2.7}$$

The term $\Delta_{ab}^{\rm sv}$ is known as the soft-virtual (SV) partonic coefficient and captures all the singular terms in the $z \to 1$ limit. Only quark-antiquark or gluon-gluon subprocesses contribute to this SV cross-section. The $\Delta_{ab}^{\rm reg}$ term contains regular (hard) contributions in the variable z. Both these contributions are expanded in a perturbative series of the strong coupling constant. In our work, we consider such an expansion up to NNLO in QCD. It is to be noted that the overall normalization factor $d\hat{\sigma}_{ab}^{(0)}/dQ$ depends on the process under study.

The singular part of the partonic coefficient has a universal structure which gets contributions from the underlying hard form factor [77–81], mass factorization kernels [82, 83] and soft radiations [84–89]. According to the KLN theorem, these infrared divergences, when regularized and combined, yield finite contributions. After the infrared cancellation, the finite part of these has the universal structure in terms of $\delta(1-z)$ and plus-distributions $\mathcal{D}_i = [\ln(1-z)^i/(1-z)]_+$. In the threshold limit, $z \to 1$, the plus distributions contribute dominantly to the SV cross section. These large distributions can be resummed to all orders in the threshold limit. Threshold resummation is conveniently performed in the Mellin (N) space where the convolution structures become simple product.

The partonic coefficient in the Mellin space is organized as follows:

$$\hat{\sigma}_N^{\text{N}^{\text{LL}}} = \int_0^1 dz \ z^{N-1} \Delta_{ab}^{\text{sv}}(z) \equiv g_0 \exp(G_N). \tag{2.8}$$

The factor g_0 is independent of the Mellin variable, whereas the threshold enhanced large logarithms ($\ln^i N$ in Mellin space) are resummed through the exponent G_N . The resummed accuracy is determined through the successive terms from the exponent G_N which up to NNLL takes the form,

$$G_N = \ln(\overline{N}) \ \bar{g}_1(\overline{N}) + \bar{g}_2(\overline{N}) + a_s \ \bar{g}_3(\overline{N}) + \dots$$
 (2.9)

where $\overline{N} = N \exp(\gamma_E)$. These coefficients are universal and only depend on the partonic flavors being either quark or gluon. Their explicit form can be found e.g. [90, 91]. In order to achieve complete resummed accuracy one also needs to know the N-independent coefficient g_0 up to sufficient accuracies. In particular, up to NNLL, it takes the form,

$$g_0 = 1 + a_s \ g_{01} + a_s^2 \ g_{02} + \dots$$
(2.10)

where $a_s = \frac{\alpha_s}{4\pi}$ and α_s is the strong coupling constant. Using the universal G_N and the process dependent g_0 , resummation for two Higgs boson production in the gluon fusion channel at N³LO + N³LL has been achieved in [92].

It is also possible to resum part (or full) of the g_0 by including them in the exponent [47, 48, 93–95], which however have subleading effect as these contributions are not dominated in the threshold region.

The N-independent coefficient g_0 is computed based on the formalism given in Ref. [96], the expression for g_{01} and g_{02} are given in Appendix A. The g_{01} requires one loop virtual computations $(\mathcal{M}_{(0,1)})$, we have computed the amplitude $\mathcal{M}_{(0,1)}$ using our in-house FORM [97] code and the expression is given in Appendix A. The full g_{02} expression requires two-loop $(\mathcal{M}_{(0,2)})$ computation as well as the one-loop squared $(\mathcal{M}_{(1,1)})$. The two loop virtual amplitude $\mathcal{M}_{(0,2)}$ are reconstructed using VVamp package [30], while the $\mathcal{M}_{(1,1)}$ is obtained by squaring $\mathcal{M}_{(0,1)}$. To obtain the results in z space, one needs to do the Mellin inversion as,

$$\frac{d\sigma^{\text{N}^{\text{nLL}}}}{dQ} = \frac{d\hat{\sigma}^{(0)}}{dQ} \sum_{a,b \in \{a,\bar{a}\}} \int_{c-i\infty}^{c+i\infty} \frac{dN}{2\pi i} \tau^{-N} f_{a,N}(\mu_F) f_{b,N}(\mu_F) \, \hat{\sigma}_N^{\text{N}^{\text{nLL}}}. \tag{2.11}$$

This complex integral contains the Landau pole at $N = \exp(1/(2a_s\beta_0) - \gamma_E)$, which makes the choice of contour very important. The Mellin inversion is performed [98] along the contour $N = c + x \exp(i\phi)$, where x is real variable. Following the minimal prescription [99], we choose the value of c such that all the singularities except the Landau pole lies on the left side of the integration contour. For numerical results we choose c = 1.9 and $\phi = 3\pi/4$.

Finally, the matched results can be written as,

$$\frac{d\sigma^{\text{N}^{\text{n}}\text{LO}+\text{N}^{\text{n}}\text{LL}}}{dQ} = \frac{d\sigma^{\text{N}^{\text{n}}\text{LO}}}{dQ} + \frac{d\hat{\sigma}^{(0)}}{dQ} \sum_{a,b \in \{q,\bar{q}\}} \int_{c-i\infty}^{c+i\infty} \frac{dN}{2\pi i} \tau^{-N} f_{a,N}(\mu_F) f_{b,N}(\mu_F) \times \left(\hat{\sigma}_N^{\text{N}^{\text{n}}\text{LL}} - \hat{\sigma}_N^{\text{N}^{\text{n}}\text{LL}} \Big|_{\text{tr}}\right).$$
(2.12)

In above equation, $f_{a,N}$ are the Mellin transformed PDF, which one can obtain using publicly available code like QCD-PEGASUS [98]. However, for numerical applications, it can also be approximated by employing the z-space PDF following [90, 100]. The last term in the bracket of Eq. (2.12) indicates the truncation of the resummed partonic coefficient Eq. (2.8), which avoids double counting the regular terms already present in the fixed order.

3 Numerical Results

In this section, we present the numerical results for the Z-boson pair production process at the LHC. For the numerical computation, we take the fine structure constant to be $\alpha=1/132.233193$. The mass of the weak gauge bosons $m_z=91.1876$ GeV, $m_w=80.385$ GeV. The Weinberg angle is $\sin^2\theta_{\rm w}=(1-m_w^2/m_z^2)=0.222897223$. This corresponds to the weak coupling $G_F=1.166379\times10^{-5}$ GeV⁻². The default choice of centre mass energy of the incoming protons is 13.6 TeV. Unless specified otherwise, in our numerical analysis, we use MSHT20 [101] parton distribution functions (PDFs) throughout taken from the LHAPDF [102]. The LO, NLO and NNLO cross-sections are obtained by convoluting the respective coefficient functions with MSHT20lo_as130, MSHT20nlo_as120 PDFs and MSHT20nnlo_as118 PDF sets, using the central set (iset=0) as the default choice. The strong coupling constant a_s is taken from LHAPDF [102], and it varies order by order in the perturbation theory. For our analysis, we consider the number of light quark flavours as $n_f=5$. For the fixed order calculations, we have used the package MATRIX [103], and the resummation results are obtained using the in-house developed code. We have used handyG [104] for numerical evaluations.

The unphysical renormalization and factorization scales are chosen to be $\mu_R = \mu_F = Q$, where Q is the invariant mass of the Z-boson pair production in the final state. The scale uncertainties are estimated by varying the unphysical scales in the range so that $|\ln(\mu_R/\mu_F)| \leq \ln 2$. The symmetric scale uncertainty is calculated from the maximum of the absolute deviation of the cross-section from that obtained with the central/default scale choice. To estimate the impact of the higher-order corrections from FO and resummation, we define the following ratios of the cross-sections which are useful in the experimental analysis:

$$K_{ij} = \frac{\sigma_{N^iLO}}{\sigma_{N^jLO}}, \ R_{ij} = \frac{\sigma_{N^iLO+N^iLL}}{\sigma_{N^jLO}} \ \text{ and } \ L_{ij} = \frac{\sigma_{N^iLO+N^iLL}}{\sigma_{N^jLO+N^jLL}} \ \text{with } i, j = 0, 1 \text{ and } 2 \cdot \quad (3.1)$$

In Fig. [1], we present the fixed order results for the invariant mass distribution of the Z-boson pair production from $2m_z$ to 1000 GeV up to NNLO in QCD. For the range of Q-variation considered here, the distribution varies over more than two orders of magnitude. In the lower panel, the corresponding fixed order K-factors, as defined in Eq. (3.1), namely K_{10} and K_{20} are given. The NLO K-factor K_{10} here varies from about 1.22 at Q = 200 GeV to about 1.55 at Q = 1000 GeV. As can be seen from Fig. [1], the variation of K_{10} above Q = 500 GeV is mild. However, the NNLO K-factor K_{20} slowly but continuously increases from about 1.29 to about 1.83 for the Q range considered here. This clearly shows additional

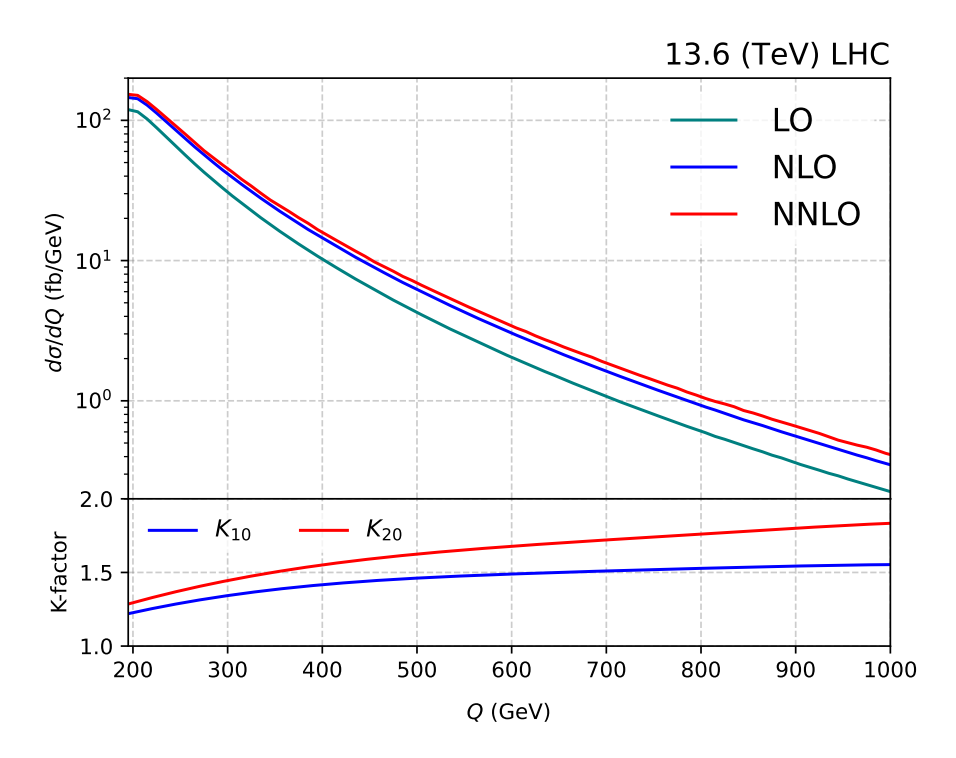


Figure 1. Fixed order invariant mass distribution for Z-boson pair production.

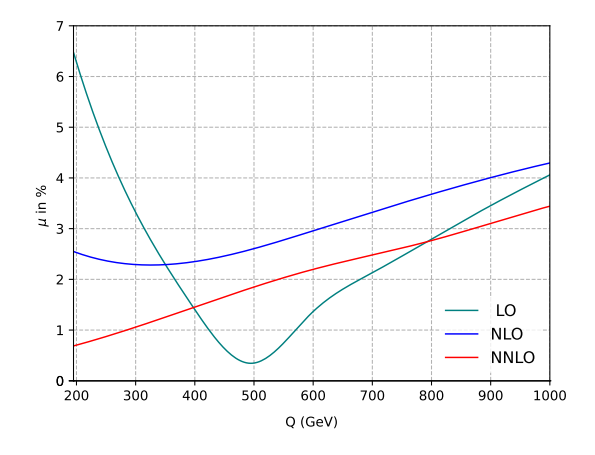


Figure 2. Fixed order 7-point scale variation for Z-boson pair production.

contributions coming from second order corrections in the higher Q-region, which are due to the real correction subprocesses like $qq' \to ZZqq'$. A more detailed discussion of this kind of contribution can be found in the Ref. [74]. The underlying theory uncertainties in these distributions up to NNLO due to the variation of arbitrary factorization and renormalization scales are presented in Fig. [2] and Fig. [3]. In Fig. [2], the complete 7-point scale variations, as discussed in the text, have been presented where the maximum uncertainty in the low Q-region at LO is as big as 6.5%. However, the inclusion of higher

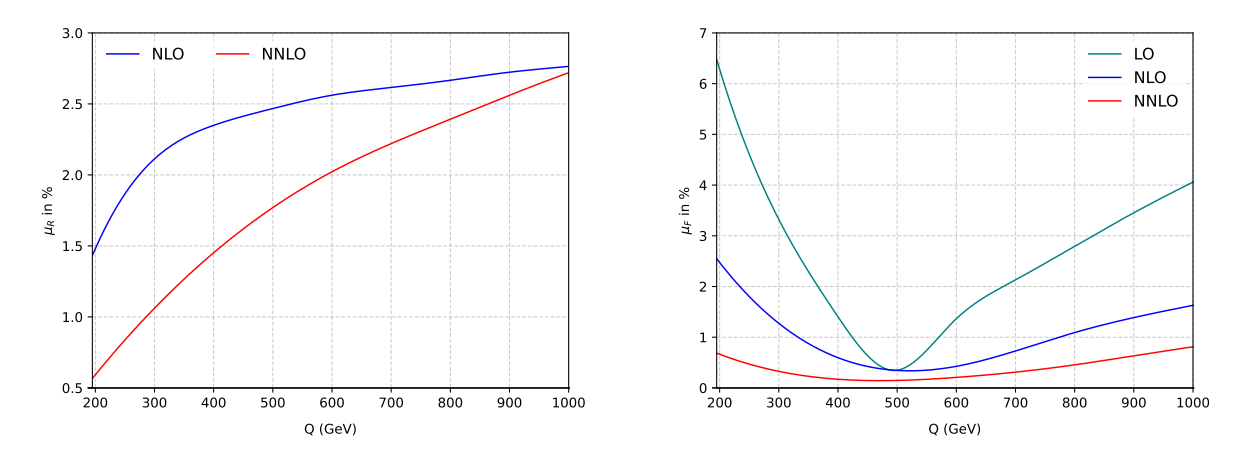


Figure 3. Fixed order μ_R and μ_F variation for Z-boson pair production.

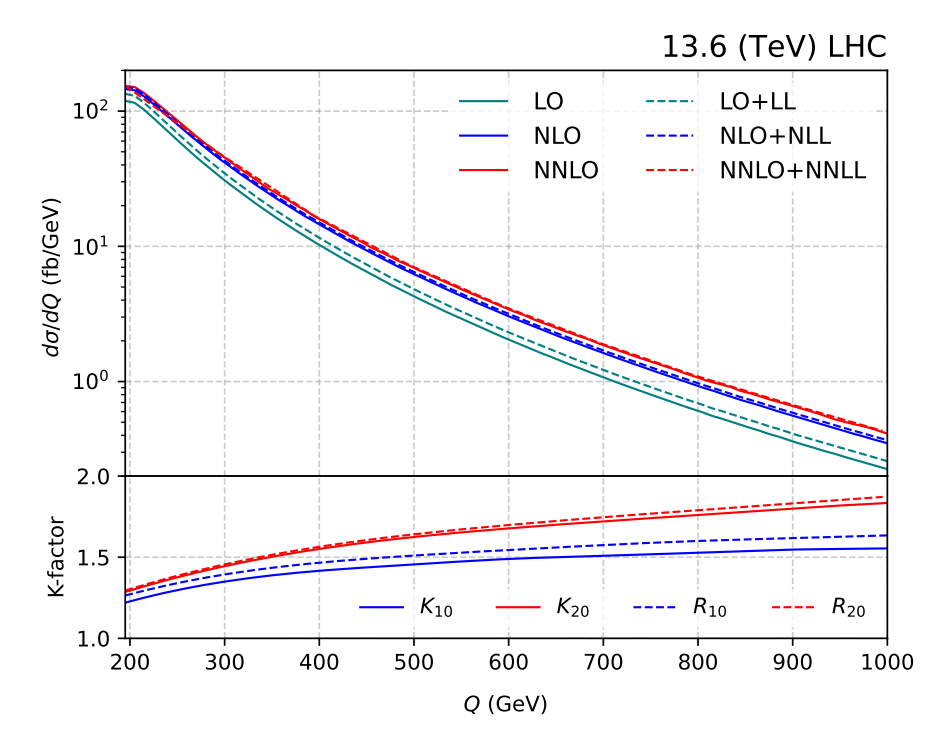


Figure 4. Fixed order and resummed invariant mass distribution for Z-boson pair production.

order NLO and NNLO corrections reduces this uncertainty to as low as 2.6% at NLO and to less than 1.0% for Q=200 GeV. The general observation is that these scale uncertainties at higher orders are found to increase with Q, which for the NNLO case are found to change from about 0.7% to about 3.4%. In the left panel of Fig. [3], we present the uncertainties due to only the renormalization scale by keeping the $\mu_F=Q$ fixed. Similarly, in the right panel, the uncertainties due to only factorization scale variations for fixed $\mu_R=Q$ are given.

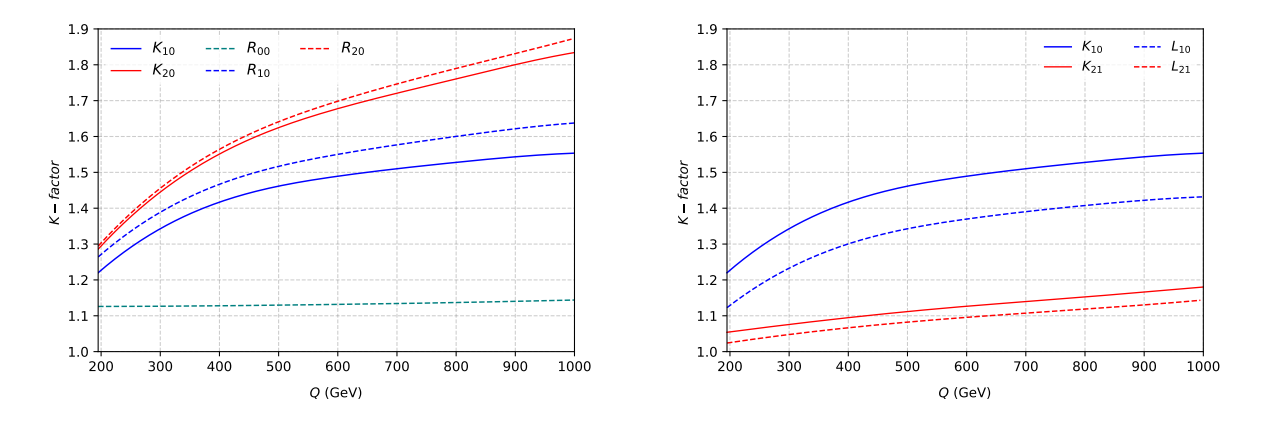


Figure 5. Fixed order and resummed K-factor for Z-boson pair production.

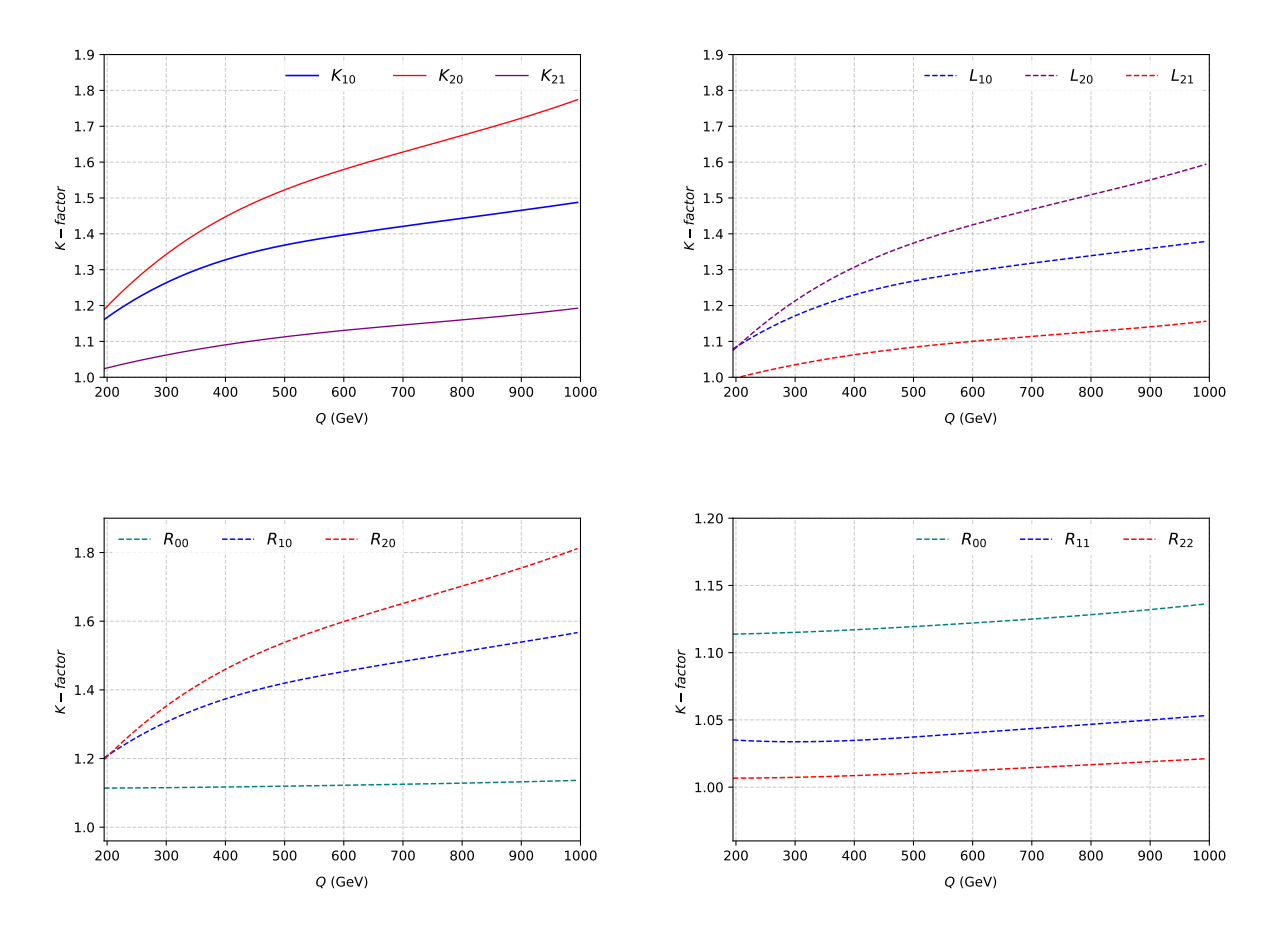


Figure 6. Fixed order and resummed K-factor with NNLO PDF for Z-boson pair production.

Next, we present the resummed cross sections to NNLO+NNLL accuracy in Fig. [4], along with the corresponding resummed K-factors K_{10} , K_{20} , R_{10} and R_{20} as defined in Eq. (3.1). The resummation has been achieved in the Mellin space where large logarithms of kind $\ln(\bar{N})$ have been resummed to NNLL accuracy as outlined in the text. We observe

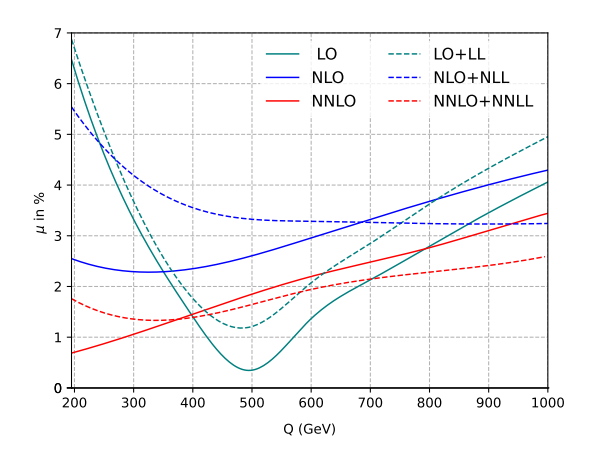


Figure 7. Fixed order and resummed 7-point scale viriation for Z-boson pair production.

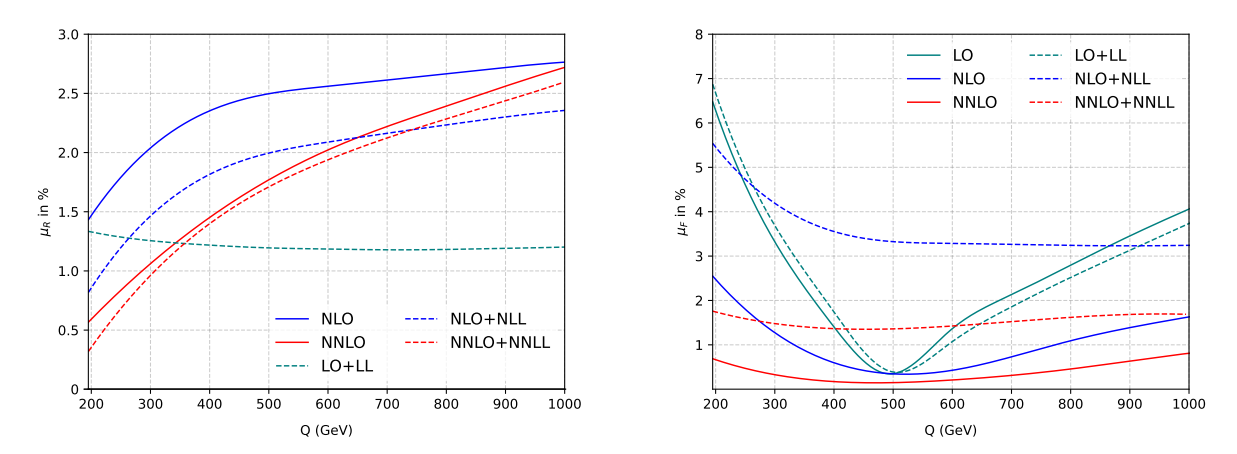


Figure 8. Fixed order and resummed μ_R and μ_F variation for Z-boson pair production.

that R_{10} varies from 1.26 to 1.64 while the R_{20} changes from 1.29 to 1.87.

To better estimate the size of higher order corrections beyond a certain fixed order as well as that of resummed contributions at different logarithmic accuracy, we present various K-factors in Fig. [5]. In the left panel of Fig. [5], we present various K_{i0} and R_{i0} for i=0,1 and 2. From R_{00} , we see that the LL resummation enhances the LO results by about 14% for Q=1000 GeV. While the NLO corrections are as big as 55%, the corresponding NLO+NLL results are about 64% of LO for the same Q region. The corresponding contribution from NNLO is about 83% where the NNLL resummation adds an additional few percent, making the NNLO+NNLL contributions sizable, about 87% of LO.

In the right panel of Fig. [5], we show K_{ij} and contrast them with the corresponding L_{ij} . We notice that, in general, L_{ij} are smaller compared to the respective K_{ij} , indicating that the threshold logarithms of a given accuracy (LL, NLL ...) capture a substantial contribution of the higher order corrections. Moreover, we notice that the gap between

 K_{21} and L_{21} is smaller than that between K_{10} and L_{10} , demonstrating a nice convergence of the higher order QCD corrections. Further, it is evident that the former gap is almost independent of Q while the latter gap increases with Q. We also notice that while the L_{10} is about as large as 1.43, the L_{21} is smaller and is about 1.14. This indicates that the contribution of the second order terms and the tower of further sub-leading logarithms (NNLL) that are not included in NLO+NLL are about 14% of NLO+NLL, and are still non-negligible for precision studies.

To study the convergence of the perturbation series, it is useful to keep the PDFs fixed and study how the cross sections vary at different orders. For this, we present the K-factors obtained from the invariant mass distribution computed with NNLO PDFs, to NNLO+NNLL accuracy. Thus, the same a_s is used both at NLO and NNLO. In the top left panel of Fig. [6], we present the fixed order K-factors, K_{10} , K_{20} and K_{21} . For a faster converging perturbation series, the factor $K_{i,i-1}$ is supposed to be as close to unity as possible. While the K_{10} has the usual NLO K-factor information and is as large as 49%, from the K_{21} we see that the NNLO corrections could contribute an additional 19% of NLO results. From the behaviour of K_{21} , we see that the second-order corrections are small, but they increase with Q. Similar results are presented but for L_{ij} in the top right panel of Fig. [6]. By definition, these ratios will estimate the contribution of higher order corrections over and above at least LO+LL level. Hence, these are smaller than the corresponding fixed order K-factors K_{ij} . In the bottom left panel of Fig. [6], we present the resummed K-factors R_{i0} to estimate the size of the resummed results above the LO predictions. We notice that the difference $(R_{20} - R_{10})$ is less than $(R_{10} - R_{00})$ for the whole invariant mass region considered here. In the bottom right panel of Fig. [6], we plot R_{ii} that gives the information about the resummed contributions over and above the corresponding fixed order corrections. We notice that the contribution from the resummed corrections for any given i is smooth but slowly increasing as Q increases. From R_{22} , we can estimate the size of higher logarithmic terms beyond NNLO to be around 2.1% of NNLO for Q = 1000 GeV.

Finally, we consider the conventional seven-point scale variations in our resummed predictions to NNLO+NNLL accuracy and present the same in Fig. [7]. We note that at LO there is no renormalization scale dependence as the underlying Born process is an electroweak process, while at LO+LL the scale μ_R enters through the tower of dominant leading logarithms to all orders, and hence the observed larger uncertainties for LO+LL compared to LO. However, at higher orders and for higher Q values, the threshold logarithms are dominant and as a result of resummation, the corresponding scale uncertainties are expected to be smaller than those in the FO ones. For the present case, the scale uncertainties at NLO+NLL (NNLO+NNLL) become smaller than those at NLO(NNLO) for Q = 700(400) GeV. While for NNLO, the scale variation reaches up to 3.4% in high Q regions, the corresponding increase for NNLO+NNLL is about 2.6%.

It is also worth noting that while performing the resummation, the large partonic threshold logarithms are resummed to all orders in the perturbation series that is expanded in a_s , and hence the uncertainties due to μ_R are expected to be smaller for a given μ_F as shown in the left panel of Fig. [8]. However, the scale μ_F enters both the PDFs as well as the parton coefficient functions. The uncertainty due to μ_F need not decrease as a result

of resummation where the PDFs used are extracted at a particular fixed order. Such a behaviour of μ_F scale uncertainty can be seen in the right panel of Fig. [7] and has already been reported in the literature [40–44, 51–53, 55, 61, 62, 105, 106].

The total production cross sections, after integrating over the invariant mass region over the full kinematic region, for LHC energies are substantially large for the Z-boson pair production process. These production cross sections have been given in the Tab. [1] up to NNLO+NNLL accuracy, along with the theory uncertainties due to the seven-point scale variations for different centre of mass energies of the incoming protons. We notice that for any given centre of mass energy, the cross sections increase while the uncertainties decrease as we go from LO to NLO, in the fixed order case. However, the uncertainties will increase from NLO to NNLO due to the gluon fusion channel opening up from the second order in perturbation theory, and hence new contributions will add up to the renormalization scale uncertainties. The gluon fluxes for the LHC energies near the $2m_z$ region is quite large, and this gluon fusion channel contributes about 9.3% of LO Z-boson pair production at 13.6 TeV LHC energy. To systematically quantify the uncertainties in the perturbation theory, we define the second order cross section without this gluon fusion channel, and call it $NNLO_{q\bar{q}}$. The scale uncertainties in this total production cross sections, LO, NLO and NNLO_{$q\bar{q}$} are found to systematically decrease from 4.24% to 1.07% for 13.6 TeV LHC energy. This behaviour remains similar for other centre of mass energies. We notice a similar behaviour in the total production cross sections after the resummation has been performed i.e. the scale uncertainties decrease from 4.62% to 1.42%, as we go from LO+LL to NNLO+NNLL. However, the NNLO+NNLL has a somewhat larger scale uncertainty compared to the one in NNLO. This is simply because of the definition of total production cross section where the invariant mass has been integrated out from $Q_{\min} = 2m_z$ to \sqrt{S} . In the lower Q-region the contribution from other channels like qg-subprocess can not be ignored. However, with increasing Q_{\min} in the total production cross-section, the scale uncertainties in NNLO+NNLL are expected to be smaller than those in NNLO, as evident from Fig. [7]. The NLO corrections for the gluon fusion channel, in the massless quark limit, are about 68% of its LO for the current LHC energies [68]. The inclusion of massive top quark loops is found to increase this correction to about 73% [71]. Finally, at this NNLO+NNLL accuracy in the perturbation theory, the NLO EW correction for Z-boson pair production also becomes important and they are found to be around -6.2%, while the mixed NNLO QCD×EW corrections [74] are about -5.7% for 13 TeV LHC.

4 Conclusions

To summarize, we have performed the threshold resummation for the production of a pair of Z-bosons at the energies of LHC, by resumming the threshold logarithms to NNLL accuracy in QCD. The final state having two massive particles makes the process dependent one-loop and two-loop virtual corrections more difficult compared to the massless final state like di-lepton or diphoton, or one-massive final state like Higgs boson. The presence of such virtual amplitudes makes not only the fixed order computation but also the resummation a challenging task to achieve numerically. In this work, we have performed this resummation

\sqrt{S}	$13.0~{ m TeV}$	13.6 TeV	100.0 TeV
LO	$10.958 \pm 4.00\%$ pb	$11.664 \pm 4.24\%$ pb	$138.617 \pm 13.84\%$ pb
NLO	$14.380 \pm 1.92\% \text{ pb}$	$15.284 \pm 1.91\%$ pb	$169.090 \pm 5.13\% \text{ pb}$
$\mathrm{NNLO}_{qar{q}}$	$15.427 \pm 1.01\%$ pb	$16.437 \pm 1.07\%$ pb	$184.438 \pm 1.69\%$ pb
NNLO	$16.418 \pm 2.22\%$ pb	$17.521 \pm 2.30\%$ pb	$212.344 \pm 3.81\%$ pb
LO+LL	$12.353 \pm 4.37\%$ pb	$13.143 \pm 4.62\%$ pb	$153.653 \pm 14.10\%$ pb
NLO+NLL	$14.890 \pm 4.49\%$ pb	$15.824 \pm 4.56\%$ pb	$174.162 \pm 7.76\%$ pb
$NNLO_{q\bar{q}}+NNLL$	$15.527 \pm 1.39\%$ pb	$16.543 \pm 1.42\%$ pb	$185.348 \pm 2.53\%$ pb
NNLO+NNLL	$16.518 \pm 1.84\%$ pb	$17.627 \pm 1.93\%$ pb	$213.254 \pm 3.64\%$ pb

Table 1. Z-boson pair production inclusive cross section for different \sqrt{S} with 7-point scale uncertainty.

by systematically matching to the known fixed order NNLO results (from the package MATRIX) and present our phenomenological results to NNLO+NNLL accuracy for both the total production cross sections as well as for the invariant mass distribution of the Z-boson pair, for the current LHC energies, 13.0 and 13.6 TeV, as well as for the upcoming future 100 TeV collider. We notice that the NNLL resummed results in general enhance the cross sections and contribute an additional few percent to the known NNLO results. We have also presented the theory uncertainties by varying the unphysical renormalization and factorization scales from Q/2 to 2Q. We find that, after performing the resummation, the scale uncertainties of about 3.4% in NNLO cross sections get reduced to about 2.6% at NNLO+NNLL level for the invariant mass region Q=1 TeV. The availability of these resummed results are expected to augment the current physics programme of the precision studies in the context of LHC and future hadron colliders.

Acknowledgements

The research work of M.C.K. is supported by SERB Core Research Grant (CRG) under the project CRG/2021/005270. The authors would like to thank A. H. Ajjath, M. Bonvini, L. Buonocore, G. Das and V. Ravindran for useful discussions. We acknowledge National Supercomputing Mission (NSM) for providing computing resources of 'PARAM Kamrupa' at IIT Guwahati, which is implemented by C-DAC and supported by the Ministry of Electronics and Information Technology (MeitY) and Department of Science and Technology (DST), Government of India, where most of the computational work has been carried out.

A Resummation coefficients

The process-dependent g_0 coefficients defined in Eq. (2.10) are given as (defining $L_{qr} = \ln(Q^2/\mu_R^2)$, $L_{fr} = \ln(\mu_F^2/\mu_R^2)$,

$$g_{01} = 2\mathcal{K}_{(0,1)} + 2C_F \left\{ -3L_{fr} + L_{qr}^2 + \zeta_2 \right\},$$

$$g_{02} = \mathcal{K}_{(1,1)} + 2\mathcal{K}_{(0,2)} + C_F n_f \left\{ -\frac{328}{21} + \frac{2}{3}L_{fr} + \frac{112}{27}L_{qr} - \frac{20}{9}L_{qr}^2 - \frac{10}{9}\zeta_2 + \frac{16}{3}L_{fr}\zeta_2 \right.$$

$$\left. -\frac{4}{3}L_{qr}\zeta_2 + \frac{32}{3}\zeta_3 \right\} + C_F^2 \left\{ -3L_{fr} + 18L_{fr}^2 - 12L_{fr}L_{qr}^2 + 2L_{qr}^4 + 12L_{fr}\zeta_2 + 4L_{qr}^2\zeta_2 \right.$$

$$\left. + 2\zeta_2^2 - 48L_{fr}\zeta_3 \right\} + C_F \left\{ +3\beta_0 L_{fr}^2 - \frac{2}{3}\beta_0 L_{qr}^3 - 12L_{fr}\mathcal{K}_{(0,1)} + 4L_{qr}^2\mathcal{K}_{(0,1)} - 6b\beta_0\zeta_2 \right.$$

$$\left. - 2\beta_0 L_{qr}\zeta_2 + 4\mathcal{K}_{(0,1)}\zeta_2 + \frac{32}{3}\beta_0\zeta_3 \right\} + C_F C_A \left\{ +\frac{2428}{81} - \frac{17}{3}L_{fr} - \frac{808}{27}L_{qr} + \frac{134}{9}L_{qr}^2 \right.$$

$$\left. + \frac{67}{9}\zeta_2 - \frac{88}{3}L_{fr}\zeta_2 + \frac{22}{3}L_{qr}\zeta_2 - 4L_{qr}^2\zeta_2 - 12\zeta_2^2 - \frac{176}{3}\zeta_3 + 24L_{fr}\zeta_3 + 28L_{qr}\zeta_3 \right\}$$

$$\left. - (A.1)$$

Here, we define

$$\mathcal{K}_{(m,n)} = \frac{\mathcal{M}_{(m,n)}^{\text{fin}}}{\mathcal{M}_{(0,0)}} \tag{A.3}$$

where,

$$\mathcal{M}_{(m,n)}^{\text{fin}} \equiv \langle \mathcal{M}_m | \mathcal{M}_n \rangle \tag{A.4}$$

and $|\mathcal{M}_n\rangle$ represents the UV-renormalized, IR-finite virtual amplitude at the n-th order in a_s , as given in Eq. (C3) of Ref. [96]. The one loop virtual contribution for ZZ production is,

$$\mathcal{M}_{(0,1)} = a_s(\mu_R^2) \frac{\Gamma(1-\epsilon)}{\Gamma(1-2\epsilon)} (4\pi)^{\epsilon} \left(\frac{\mu_R^2}{s}\right)^{\epsilon} C_F \left[-4\left\{ \frac{1}{\epsilon^2} + \frac{3}{2\epsilon} \right\} \mathcal{M}_{(0,0)} + \mathcal{M}_{(0,1)}^f \right]. \tag{A.5}$$

here,

$$\mathcal{M}_{(0,1)}^{f} = B_f N(c_v^4 + 6c_v^2 c_a^2 + c_a^4) \left(\frac{4}{t^2 u^2}\right) \left[2\zeta_2 \left(-20m_z^2 t u(t+u) - 4m_z^4 (t^2 - 8tu + u^2) + t u(5t^2 + 4tu + 5u^2) + \frac{t u}{\kappa s (4m_z^2 - s)^2} \left(-32m_z^6 t u - 64m_z^8 (t+u) + 8m_z^2 t u(t+u)^2 - (t+u)^3 (3t^2 + 4tu + 3u^2) + m_z^4 (22t^3 + 82t^2 u + 82tu^2 + 22u^3) \right) + \ln\left(\frac{s}{m_z^2}\right) \frac{1}{(4m_z^2 - s)^2} \left(8m_z^2 t^2 u^2 (t+u) + 12m_z^8 (t^2 - 8tu + u^2) - t u(t+u)^2 (3t^2 + 4tu + 3u^2)\right) \right)$$

$$\begin{split} &+4m_z^6(3t^3-5t^2u-5tu^2+3u^3)+m_z^4(3t^4+14t^3u+78t^2u^2+14tu^3+3u^4)\\ &+\frac{tu}{\kappa s(4m_z^2-s)^2} \left(\ln(x)+4\text{Li}_2(-x)\right) \left(-32m_z^6tu-64m_z^8(t+u)\right)\\ &+8m_z^2tu(t+u)^2-(t+u)^3(3t^2+4tu+3u^2)\\ &+m_z^4(22t^3+82t^2u+82tu^2+22u^3)\right)+\frac{1}{(t-m_z^2)(u-m_z^2)(4m_z^2-s)} \left(18m_z^{10}(t^2-8tu+u^2)+m_z^8(-9t^3+131t^2u+131tu^2-9u^3)\right)\\ &-7t^2u^2(t^3+t^2u+tu^2+u^3)-4m_z^4tu(4t^3+23t^2u+23tu^2+4u^3)\\ &+m_z^6(-9t^4+14t^3u-66t^2u^2)+14tu^3-9u^4\right)\\ &+m_z^2tu(9t^4+32t^3u+82t^2u^2+32tu^3+9u^4)+\ln\left(\frac{-t}{m_z^2}\right)\frac{u}{(t-m_z^2)^2} \left(3m_z^8(-4t+u)+6m_z^6t(2t+u)-2m_z^2t^2u(4t+u)+3t^3u(2t+3u)\right)\\ &+m_z^4t(-2t^2+tu-3u^2)\right)+\left(2\ln\left(\frac{-t}{m_z^2}\right)\ln\left(\frac{t-m_z^2}{m_z^2s}\right)+4\text{Li}_2\left(\frac{t}{m_z^2}\right)\right)\\ &-\ln^2\left(\frac{-t}{m_z^2}\right)\right)u(m_z^4(8t-2u)-4m_z^2t(2t+u)+t(2t^2+2tu+u^2))\\ &+\ln\left(\frac{-u}{m_z^2}\right)\frac{t}{(u-m_z^2)^2}\left(3m_z^8(-4u+t)+6m_z^6u(2u+t)-2m_z^2u^2t(4u+t)\right)\\ &+3u^3t(2u+3t)+m_z^4u(-2u^2+tu-3t^2)\right)+\left(2\ln\left(\frac{-u}{m_z^2}\right)\ln\left(\frac{u-m_z^2}{m_z^2s}\right)\\ &+4\text{Li}_2\left(\frac{u}{m_z^2}\right)-\ln^2\left(\frac{-u}{m_z^2}\right)\right)t(m_z^4(8u-2t)-4m_z^2u(2u+t)\right)\\ &+4\text{Li}_2\left(\frac{u}{m_z^2}\right)-\ln^2\left(\frac{-u}{m_z^2}\right)\right]. \end{split}$$

$$x = \frac{1 - \kappa}{1 + \kappa}; \quad \kappa = \sqrt{1 - 4\frac{m_z^2}{s}} \tag{A.6}$$

The process-independent universal resum exponent defined in Eq. (2.9) which are used for DY-type processes are given as,

$$g_{1} = \left[\frac{A_{1}}{\beta_{0}} \left\{2 - 2\ln(1 - \omega) + 2\ln(1 - \omega) \omega^{-1}\right\}\right], \tag{A.7}$$

$$g_{2} = \left[\frac{D_{1}}{\beta_{0}} \left\{\frac{1}{2}\ln(1 - \omega)\right\} + \frac{A_{2}}{\beta_{0}^{2}} \left\{-\ln(1 - \omega) - \omega\right\} + \frac{A_{1}}{\beta_{0}} \left\{\left(\ln(1 - \omega) + \frac{1}{2}\ln(1 - \omega)^{2} + \omega\right) \left(\frac{\beta_{1}}{\beta_{0}^{2}}\right) + \left(\omega\right) L_{fr} + \left(\ln(1 - \omega)\right) L_{qr}\right\}\right], \tag{A.8}$$

$$g_{3} = \left[\frac{A_{3}}{\beta_{0}^{2}} \left\{-\frac{\omega}{(1 - \omega)} + \omega\right\} + \frac{A_{2}}{\beta_{0}} \left\{\left(2\frac{\omega}{(1 - \omega)}\right) L_{qr} + \left(3\frac{\omega}{(1 - \omega)} + 2\frac{\ln(1 - \omega)}{(1 - \omega)} - \omega\right) \left(\frac{\beta_{1}}{\beta_{0}^{2}}\right) + \left(-2\omega\right) L_{fr}\right\} + A_{1} \left\{-4\zeta_{2}\frac{\omega}{(1 - \omega)} + \left(-\frac{\ln(1 - \omega)^{2}}{(1 - \omega)} - \frac{\omega}{(1 - \omega)} - \omega\right) \left(\frac{\beta_{1}}{\beta_{0}^{2}}\right) + 2\ln(1 - \omega) + \omega\right) \left(\frac{\beta_{1}}{\beta_{0}^{2}}\right)^{2} + \left(-\frac{\omega}{(1 - \omega)}\right) L_{qr}^{2} + \left(-\frac{\omega}{(1 - \omega)}\right) L_{qr}^{$$

$$-2 \ln(1-\omega) - \omega \left(\frac{\beta_2}{\beta_0^3} \right) + \left(\left(-2 \frac{\omega}{(1-\omega)} - 2 \frac{\ln(1-\omega)}{(1-\omega)} \right) \left(\frac{\beta_1}{\beta_0^2} \right) \right) L_{qr}$$

$$+ \left(\omega \right) L_{fr}^2 \right\} + \frac{D_2}{\beta_0} \left\{ \frac{\omega}{(1-\omega)} \right\} + D_1 \left\{ \left(-\frac{\omega}{(1-\omega)} \right) L_{qr} + \left(-\frac{\omega}{(1-\omega)} \right) - \frac{\ln(1-\omega)}{(1-\omega)} \right) \left(\frac{\beta_1}{\beta_0^2} \right) \right\} \right],$$
(A.9)

Here A_i are the universal cusp anomalous dimensions, D_i are the threshold noncusp anomalous dimensions, and $\omega = 2a_s\beta_0 \ln \overline{N}$. Note that all the perturbative quantities are expanded in powers of a_s . The cusp anomalous dimensions A_i are given as (recently four-loops results are available can be found in Ref. [107–109]),

$$A_1 = C_F \left\{ 4 \right\},\tag{A.10}$$

$$A_2 = C_F \left\{ n_f \left(-\frac{40}{9} \right) + C_A \left(\frac{268}{9} - 8\zeta_2 \right) \right\},\tag{A.11}$$

$$A_{3} = C_{F} \left\{ n_{f}^{2} \left(-\frac{16}{27} \right) + C_{F} n_{f} \left(-\frac{110}{3} + 32\zeta_{3} \right) + C_{A} n_{f} \left(-\frac{836}{27} - \frac{112}{3} \zeta_{3} + \frac{160}{9} \zeta_{2} \right) + C_{A}^{2} \left(\frac{490}{3} + \frac{88}{3} \zeta_{3} - \frac{1072}{9} \zeta_{2} + \frac{176}{5} \zeta_{2}^{2} \right) \right\},$$
(A.12)

The coefficients D_i are given as,

$$D_1 = C_F \left\{ 0 \right\},\tag{A.13}$$

$$D_2 = C_F \left\{ n_f \left(\frac{224}{27} - \frac{32}{3} \zeta_2 \right) + C_A \left(-\frac{1616}{27} + 56\zeta_3 + \frac{176}{3} \zeta_2 \right) \right\},\tag{A.14}$$

Here,

$$C_A = N, \quad C_F = \frac{N^2 - 1}{2N},$$
 (A.15)

$$\beta_0 = \frac{11}{3}C_A - \frac{2}{3}n_f, \tag{A.16}$$

$$\beta_1 = \frac{34}{3}C_A^2 - \frac{10}{3}n_f C_A - 2n_f C_F, \tag{A.17}$$

$$\beta_2 = \frac{2857}{54} C_A^3 - \frac{1415}{54} n_f C_A^2 - \frac{205}{18} n_f C_F C_A + n_f C_F^2 + \frac{79}{54} n_f^2 C_A + \frac{11}{9} n_f^2 C_F.$$
 (A.18)

References

- [1] CMS collaboration, A. Tumasyan et al., Measurements of the electroweak diboson production cross sections in proton-proton collisions at $\sqrt{s} = 5.02$ TeV using leptonic decays, Phys. Rev. Lett. 127 (2021) 191801 [2107.01137].
- [2] ATLAS collaboration, G. Aad et al., Measurement of the ZZ production cross section and limits on anomalous neutral triple gauge couplings in proton-proton collisions at $\sqrt{s} = 7$ TeV with the ATLAS detector, Phys. Rev. Lett. 108 (2012) 041804 [1110.5016].

- [3] ATLAS collaboration, G. Aad et al., Measurement of ZZ production in pp collisions at $\sqrt{s} = 7$ TeV and limits on anomalous ZZZ and ZZ γ couplings with the ATLAS detector, JHEP 03 (2013) 128 [1211.6096].
- [4] CMS collaboration, S. Chatrchyan et al., Measurement of the ZZ Production Cross Section and Search for Anomalous Couplings in 2 l2l 'Final States in pp Collisions at $\sqrt{s} = 7$ TeV, JHEP 01 (2013) 063 [1211.4890].
- [5] CMS collaboration, V. Khachatryan et al., Measurements of the Z Z production cross sections in the $2l2\nu$ channel in proton-proton collisions at $\sqrt{s} = 7$ and 8 TeV and combined constraints on triple gauge couplings, Eur. Phys. J. C 75 (2015) 511 [1503.05467].
- [6] CMS collaboration, S. Chatrchyan et al., Measurement of W^+W^- and ZZ Production Cross Sections in pp Collisions at $\sqrt{s} = 8TeV$, Phys. Lett. B **721** (2013) 190 [1301.4698].
- [7] CMS collaboration, V. Khachatryan et al., Measurement of the $pp \to ZZ$ Production Cross Section and Constraints on Anomalous Triple Gauge Couplings in Four-Lepton Final States at $\sqrt{s} = 8$ TeV, Phys. Lett. B 740 (2015) 250 [1406.0113].
- [8] ATLAS collaboration, G. Aad et al., Measurements of four-lepton production in pp collisions at $\sqrt{s} = 8$ TeV with the ATLAS detector, Phys. Lett. B **753** (2016) 552 [1509.07844].
- [9] ATLAS collaboration, M. Aaboud et al., Measurement of the ZZ production cross section in proton-proton collisions at $\sqrt{s} = 8$ TeV using the $ZZ \to \ell^-\ell^+\ell'^-\ell'^+$ and $ZZ \to \ell^-\ell^+\nu\bar{\nu}$ channels with the ATLAS detector, JHEP 01 (2017) 099 [1610.07585].
- [10] CMS collaboration, A. M. Sirunyan et al., Measurement of differential cross sections for Z boson pair production in association with jets at $\sqrt{s} = 8$ and 13 TeV, Phys. Lett. B 789 (2019) 19 [1806.11073].
- [11] CMS collaboration, V. Khachatryan et al., Measurement of the ZZ production cross section and $Z \to \ell^+ \ell^- \ell'^+ \ell'^-$ branching fraction in pp collisions at \sqrt{s} =13 TeV, Phys. Lett. B **763** (2016) 280 [1607.08834].
- [12] ATLAS collaboration, M. Aaboud et al., $ZZ \to \ell^+\ell^-\ell'^+\ell'^-$ cross-section measurements and search for anomalous triple gauge couplings in 13 TeV pp collisions with the ATLAS detector, Phys. Rev. D 97 (2018) 032005 [1709.07703].
- [13] CMS collaboration, A. M. Sirunyan et al., Measurements of the pp \rightarrow ZZ production cross section and the Z \rightarrow 4 ℓ branching fraction, and constraints on anomalous triple gauge couplings at $\sqrt{s} = 13$ TeV, Eur. Phys. J. C 78 (2018) 165 [1709.08601].
- [14] ATLAS collaboration, M. Aaboud et al., Measurement of ZZ production in the $\ell\ell\nu\nu$ final state with the ATLAS detector in pp collisions at $\sqrt{s}=13$ TeV, JHEP 10 (2019) 127 [1905.07163].
- [15] CMS collaboration, A. M. Sirunyan et al., Measurements of pp \rightarrow ZZ production cross sections and constraints on anomalous triple gauge couplings at $\sqrt{s} = 13$ TeV, Eur. Phys. J. C 81 (2021) 200 [2009.01186].
- [16] ATLAS collaboration, G. Aad et al., Measurement of zz production cross-sections in the four-lepton final state in pp collisions at s=13.6tev with the atlas experiment, Physics Letters B 855 (2024) 138764.
- [17] J. Ohnemus and J. F. Owens, Order- α_s calculation of hadronic zz production, Phys. Rev. D 43 (1991) 3626.

- [18] B. Mele, P. Nason and G. Ridolfi, QCD radiative corrections to Z boson pair production in hadronic collisions, Nucl. Phys. B 357 (1991) 409.
- [19] C. Zecher, T. Matsuura and J. J. van der Bij, Leptonic signals from off-shell Z boson pairs at hadron colliders, Z. Phys. C 64 (1994) 219 [hep-ph/9404295].
- [20] J. Ohnemus, Hadronic ZZ, W⁻W⁺, and W[±]Z production with QCD corrections and leptonic decays, Phys. Rev. D **50** (1994) 1931 [hep-ph/9403331].
- [21] J. M. Campbell and R. K. Ellis, An Update on vector boson pair production at hadron colliders, Phys. Rev. D 60 (1999) 113006 [hep-ph/9905386].
- [22] L. J. Dixon, Z. Kunszt and A. Signer, Helicity amplitudes for O(alpha-s) production of W^+W^- , $W^\pm Z$, ZZ, $W^\pm \gamma$, or $Z\gamma$ pairs at hadron colliders, Nucl. Phys. B **531** (1998) 3 [hep-ph/9803250].
- [23] J. M. Campbell, R. K. Ellis and C. Williams, Vector Boson Pair Production at the LHC, JHEP 07 (2011) 018 [1105.0020].
- [24] T. Melia, P. Nason, R. Rontsch and G. Zanderighi, W+W-, WZ and ZZ production in the POWHEG BOX, JHEP 11 (2011) 078 [1107.5051].
- [25] P. Nason and G. Zanderighi, W^+W^- , WZ and ZZ production in the POWHEG-BOX-V2, Eur. Phys. J. C **74** (2014) 2702 [1311.1365].
- [26] R. Frederix, S. Frixione, V. Hirschi, F. Maltoni, R. Pittau and P. Torrielli, Four-lepton production at hadron colliders: aMC@NLO predictions with theoretical uncertainties, JHEP 02 (2012) 099 [1110.4738].
- [27] N. Agarwal, V. Ravindran, V. K. Tiwari and A. Tripathi, Z boson pair production at the LHC to O(alpha(s)) in TeV scale gravity models, Nucl. Phys. B 830 (2010) 248 [0909.2651].
- [28] T. Binoth, T. Gleisberg, S. Karg, N. Kauer and G. Sanguinetti, NLO QCD corrections to ZZ+ jet production at hadron colliders, Phys. Lett. B 683 (2010) 154 [0911.3181].
- [29] F. Campanario, M. Kerner, L. D. Ninh and D. Zeppenfeld, Next-to-leading order QCD corrections to ZZ production in association with two jets, JHEP 07 (2014) 148 [1405.3972].
- [30] T. Gehrmann, A. von Manteuffel and L. Tancredi, The two-loop helicity amplitudes for $q\overline{q}' \to V_1V_2 \to 4$ leptons, JHEP **09** (2015) 128 [1503.04812].
- [31] F. Cascioli, T. Gehrmann, M. Grazzini, S. Kallweit, P. Maierhöfer, A. von Manteuffel et al., ZZ production at hadron colliders in NNLO QCD, Phys. Lett. B 735 (2014) 311 [1405.2219].
- [32] G. Heinrich, S. Jahn, S. P. Jones, M. Kerner and J. Pires, NNLO predictions for Z-boson pair production at the LHC, JHEP 03 (2018) 142 [1710.06294].
- [33] M. Grazzini, S. Kallweit and D. Rathlev, ZZ production at the LHC: fiducial cross sections and distributions in NNLO QCD, Phys. Lett. B 750 (2015) 407 [1507.06257].
- [34] S. Kallweit and M. Wiesemann, ZZ production at the LHC: NNLO predictions for $2\ell 2\nu$ and 4ℓ signatures, Phys. Lett. B **786** (2018) 382 [1806.05941].
- [35] M. Grazzini, S. Kallweit, D. Rathlev and M. Wiesemann, $W^{\pm}Z$ production at the LHC: fiducial cross sections and distributions in NNLO QCD, JHEP **05** (2017) 139 [1703.09065].
- [36] C. Duhr, F. Dulat and B. Mistlberger, *Drell-Yan Cross Section to Third Order in the Strong Coupling Constant*, *Phys. Rev. Lett.* **125** (2020) 172001 [2001.07717].

- [37] C. Duhr, F. Dulat and B. Mistlberger, Charged current Drell-Yan production at N³LO, JHEP 11 (2020) 143 [2007.13313].
- [38] C. Duhr and B. Mistlberger, Lepton-pair production at hadron colliders at N³LO in QCD, JHEP 03 (2022) 116 [2111.10379].
- [39] J. Baglio, C. Duhr, B. Mistlberger and R. Szafron, Inclusive production cross sections at N³LO, JHEP 12 (2022) 066 [2209.06138].
- [40] A. A H, G. Das, M. C. Kumar, P. Mukherjee, V. Ravindran and K. Samanta, Resummed Drell-Yan cross-section at N³LL, JHEP 10 (2020) 153 [2001.11377].
- [41] G. Das, C. Dey, M. C. Kumar and K. Samanta, Threshold enhanced cross sections for colorless productions, Phys. Rev. D 107 (2023) 034038 [2210.17534].
- [42] G. Das, C. Dey, M. C. Kumar and K. Samanta, Precision Studies for Higgs-Strahlung Process at Hadron Collider, Springer Proc. Phys. 304 (2024) 245.
- [43] A. A H, P. Mukherjee and V. Ravindran, Next to soft corrections to Drell-Yan and Higgs boson productions, Phys. Rev. D 105 (2022) 094035 [2006.06726].
- [44] A. A H, P. Mukherjee, V. Ravindran, A. Sankar and S. Tiwari, Next-to SV resummed Drell-Yan cross section beyond leading-logarithm, Eur. Phys. J. C 82 (2022) 234 [2107.09717].
- [45] C. Anastasiou, C. Duhr, F. Dulat, F. Herzog and B. Mistlberger, Higgs Boson Gluon-Fusion Production in QCD at Three Loops, Phys. Rev. Lett. 114 (2015) 212001 [1503.06056].
- [46] F. Dulat, B. Mistlberger and A. Pelloni, Differential Higgs production at N³LO beyond threshold, JHEP 01 (2018) 145 [1710.03016].
- [47] M. Bonvini and S. Marzani, Resummed Higgs cross section at N³LL, JHEP 09 (2014) 007 [1405.3654].
- [48] M. Bonvini, S. Marzani, C. Muselli and L. Rottoli, On the Higgs cross section at N^3LO+N^3LL and its uncertainty, JHEP 08 (2016) 105 [1603.08000].
- [49] T. Ahmed, M. C. Kumar, P. Mathews, N. Rana and V. Ravindran, Pseudo-scalar Higgs boson production at threshold N³ LO and N³ LL QCD, Eur. Phys. J. C 76 (2016) 355 [1510.02235].
- [50] T. Ahmed, M. Bonvini, M. C. Kumar, P. Mathews, N. Rana, V. Ravindran et al., Pseudo-scalar Higgs boson production at N³ LO_A +N³ LL', Eur. Phys. J. C 76 (2016) 663 [1606.00837].
- [51] A. A H, P. Mukherjee, V. Ravindran, A. Sankar and S. Tiwari, Resummed Higgs boson cross section at next-to SV to NNLO + NNLL, Eur. Phys. J. C 82 (2022) 774 [2109.12657].
- [52] A. Bhattacharya, M. C. Kumar, P. Mathews and V. Ravindran, Next-to-soft-virtual resummed prediction for pseudoscalar Higgs boson production at NNLO+NNLL⁻, Phys. Rev. D 105 (2022) 116015 [2112.02341].
- [53] A. A. H., A. Chakraborty, G. Das, P. Mukherjee and V. Ravindran, Resummed prediction for Higgs boson production through b\overline{b} annihilation at N³LL, JHEP 11 (2019) 006 [1905.03771].
- [54] G. Das and A. Sankar, Next-to-soft threshold effects on Higgs boson production via bottom quark annihilation, 2409.01553.

- [55] P. Banerjee, G. Das, P. K. Dhani and V. Ravindran, Threshold resummation of the rapidity distribution for Drell-Yan production at NNLO+NNLL, Phys. Rev. D 98 (2018) 054018 [1805.01186].
- [56] G. Das, Z, W^{\pm} rapidity distributions at NNLL and beyond, 2303.16578.
- [57] A. A H, P. Mukherjee, V. Ravindran, A. Sankar and S. Tiwari, Next-to-soft corrections for Drell-Yan and Higgs boson rapidity distributions beyond N³LO, Phys. Rev. D 103 (2021) L111502 [2010.00079].
- [58] T. Ahmed, A. A H, P. Mukherjee, V. Ravindran and A. Sankar, Rapidity distribution at soft-virtual and beyond for n-colorless particles to N⁴LO in QCD, Eur. Phys. J. C 81 (2021) 943 [2010.02980].
- [59] A. A H, P. Mukherjee, V. Ravindran, A. Sankar and S. Tiwari, Next-to-soft-virtual resummed rapidity distribution for the Drell-Yan process to NNLO+NNLL⁻, Phys. Rev. D 106 (2022) 034005 [2112.14094].
- [60] V. Ravindran, A. Sankar and S. Tiwari, Rapidity distribution of pseudoscalar Higgs boson to NNLOA+NNLL, Phys. Rev. D 110 (2024) 016019 [2309.14833].
- [61] P. Banerjee, G. Das, P. K. Dhani and V. Ravindran, Threshold resummation of the rapidity distribution for Higgs production at NNLO+NNLL, Phys. Rev. D 97 (2018) 054024 [1708.05706].
- [62] V. Ravindran, A. Sankar and S. Tiwari, Resummed next-to-soft corrections to rapidity distribution of Higgs boson to NNLO+NNLL, Phys. Rev. D 108 (2023) 014012 [2205.11560].
- [63] G. Das, Higgs boson rapidity distribution in bottom annihilation at NNLL and beyond, Phys. Rev. D 108 (2023) 094028 [2306.04561].
- [64] M. Grazzini, S. Kallweit, D. Rathlev and M. Wiesemann, Transverse-momentum resummation for vector-boson pair production at NNLL+NNLO, JHEP 08 (2015) 154 [1507.02565].
- [65] J. M. Campbell, R. K. Ellis, T. Neumann and S. Seth, Transverse momentum resummation at N³LL+NNLO for diboson processes, JHEP 03 (2023) 080 [2210.10724].
- [66] L. Buonocore, G. Koole, D. Lombardi, L. Rottoli, M. Wiesemann and G. Zanderighi, ZZ production at nNNLO+PS with MiNNLO_{PS}, JHEP 01 (2022) 072 [2108.05337].
- [67] T. Binoth, N. Kauer and P. Mertsch, Gluon-induced QCD corrections to pp —> ZZ —> l anti-l l-prime anti-l-prime, in 16th International Workshop on Deep Inelastic Scattering and Related Subjects, p. 142, 7, 2008, 0807.0024, DOI.
- [68] F. Caola, K. Melnikov, R. Röntsch and L. Tancredi, QCD corrections to ZZ production in gluon fusion at the LHC, Phys. Rev. D 92 (2015) 094028 [1509.06734].
- [69] M. Grazzini, S. Kallweit, M. Wiesemann and J. Y. Yook, ZZ production at the LHC: NLO QCD corrections to the loop-induced gluon fusion channel, JHEP 03 (2019) 070 [1811.09593].
- [70] M. Grazzini, S. Kallweit, M. Wiesemann and J. Y. Yook, Four lepton production in gluon fusion: Off-shell Higgs effects in NLO QCD, Phys. Lett. B 819 (2021) 136465 [2102.08344].
- [71] B. Agarwal, S. Jones, M. Kerner and A. von Manteuffel, Complete NLO QCD Corrections to ZZ Production in Gluon Fusion, 2404.05684.

- [72] S. Alioli, F. Caola, G. Luisoni and R. Röntsch, ZZ production in gluon fusion at NLO matched to parton-shower, Phys. Rev. D 95 (2017) 034042 [1609.09719].
- [73] A. Bierweiler, T. Kasprzik and J. H. Kühn, Vector-boson pair production at the LHC to $\mathcal{O}(\alpha^3)$ accuracy, JHEP 12 (2013) 071 [1305.5402].
- [74] M. Grazzini, S. Kallweit, J. M. Lindert, S. Pozzorini and M. Wiesemann, NNLO QCD + NLO EW with Matrix+OpenLoops: precise predictions for vector-boson pair production, JHEP 02 (2020) 087 [1912.00068].
- [75] A. Denner and G. Pelliccioli, NLO EW and QCD corrections to polarized ZZ production in the four-charged-lepton channel at the LHC, JHEP 10 (2021) 097 [2107.06579].
- [76] Y. Wang, C. S. Li, Z. L. Liu and D. Y. Shao, Threshold resummation for W[±]Z and ZZ pair production at the LHC, Phys. Rev. D 90 (2014) 034008 [1406.1417].
- [77] S. Moch, J. A. M. Vermaseren and A. Vogt, Three-loop results for quark and gluon form-factors, Phys. Lett. B 625 (2005) 245 [hep-ph/0508055].
- [78] S. Moch, J. A. M. Vermaseren and A. Vogt, *The Quark form-factor at higher orders*, *JHEP* **08** (2005) 049 [hep-ph/0507039].
- [79] P. A. Baikov, K. G. Chetyrkin, A. V. Smirnov, V. A. Smirnov and M. Steinhauser, Quark and gluon form factors to three loops, Phys. Rev. Lett. 102 (2009) 212002 [0902.3519].
- [80] T. Gehrmann, E. W. N. Glover, T. Huber, N. Ikizlerli and C. Studerus, Calculation of the quark and gluon form factors to three loops in QCD, JHEP 06 (2010) 094 [1004.3653].
- [81] T. Gehrmann and D. Kara, The $Hb\bar{b}$ form factor to three loops in QCD, JHEP **09** (2014) 174 [1407.8114].
- [82] S. Moch, J. A. M. Vermaseren and A. Vogt, The Three loop splitting functions in QCD: The Nonsinglet case, Nucl. Phys. B 688 (2004) 101 [hep-ph/0403192].
- [83] A. Vogt, S. Moch and J. A. M. Vermaseren, The Three-loop splitting functions in QCD: The Singlet case, Nucl. Phys. B 691 (2004) 129 [hep-ph/0404111].
- [84] V. Ravindran, On Sudakov and soft resummations in QCD, Nucl. Phys. B 746 (2006) 58 [hep-ph/0512249].
- [85] V. Ravindran, Higher-order threshold effects to inclusive processes in QCD, Nucl. Phys. B 752 (2006) 173 [hep-ph/0603041].
- [86] V. V. Sudakov, Vertex parts at very high-energies in quantum electrodynamics, Sov. Phys. JETP 3 (1956) 65.
- [87] A. H. Mueller, On the Asymptotic Behavior of the Sudakov Form-factor, Phys. Rev. D 20 (1979) 2037.
- [88] J. C. Collins, Algorithm to Compute Corrections to the Sudakov Form-factor, Phys. Rev. D 22 (1980) 1478.
- [89] A. Sen, Asymptotic Behavior of the Sudakov Form-Factor in QCD, Phys. Rev. D 24 (1981) 3281.
- [90] S. Catani, D. de Florian, M. Grazzini and P. Nason, Soft gluon resummation for Higgs boson production at hadron colliders, JHEP 07 (2003) 028 [hep-ph/0306211].
- [91] S. Moch, J. A. M. Vermaseren and A. Vogt, Higher-order corrections in threshold resummation, Nucl. Phys. B 726 (2005) 317 [hep-ph/0506288].

- [92] A. A H and H.-S. Shao, N^3LO+N^3LL QCD improved Higgs pair cross sections, JHEP **02** (2023) 067 [2209.03914].
- [93] T. O. Eynck, E. Laenen and L. Magnea, Exponentiation of the Drell-Yan cross-section near partonic threshold in the DIS and MS-bar schemes, JHEP 06 (2003) 057 [hep-ph/0305179].
- [94] G. Das, S.-O. Moch and A. Vogt, Soft corrections to inclusive deep-inelastic scattering at four loops and beyond, JHEP 03 (2020) 116 [1912.12920].
- [95] A. H. Ajjath, G. Das, M. C. Kumar, P. Mukherjee, V. Ravindran and K. Samanta, Resummed Drell-Yan cross-section at N³LL, JHEP 10 (2020) 153 [2001.11377].
- [96] T. Ahmed, A. H. Ajjath, G. Das, P. Mukherjee, V. Ravindran and S. Tiwari, Soft-virtual correction and threshold resummation for n-colorless particles to fourth order in QCD: Part I, 2010.02979.
- [97] B. Ruijl, T. Ueda and J. A. M. Vermaseren, FORM version 4.2, 1707.06453.
- [98] A. Vogt, Efficient evolution of unpolarized and polarized parton distributions with QCD-PEGASUS, Comput. Phys. Commun. 170 (2005) 65 [hep-ph/0408244].
- [99] S. Catani, M. L. Mangano, P. Nason and L. Trentadue, The Resummation of soft gluons in hadronic collisions, Nucl. Phys. B 478 (1996) 273 [hep-ph/9604351].
- [100] S. Catani and L. Trentadue, Resummation of the QCD Perturbative Series for Hard Processes, Nucl. Phys. B 327 (1989) 323.
- [101] S. Bailey, T. Cridge, L. A. Harland-Lang, A. D. Martin and R. S. Thorne, Parton distributions from LHC, HERA, Tevatron and fixed target data: MSHT20 PDFs, Eur. Phys. J. C 81 (2021) 341 [2012.04684].
- [102] A. Buckley, J. Ferrando, S. Lloyd, K. Nordström, B. Page, M. Rüfenacht et al., LHAPDF6: parton density access in the LHC precision era, Eur. Phys. J. C 75 (2015) 132 [1412.7420].
- [103] M. Grazzini, S. Kallweit and M. Wiesemann, Fully differential NNLO computations with MATRIX, Eur. Phys. J. C 78 (2018) 537 [1711.06631].
- [104] L. Naterop, A. Signer and Y. Ulrich, handyG—Rapid numerical evaluation of generalised polylogarithms in Fortran, Comput. Phys. Commun. 253 (2020) 107165 [1909.01656].
- [105] G. Das, M. C. Kumar and K. Samanta, Resummed inclusive cross-section in ADD model at N³LL, JHEP 10 (2020) 161 [1912.13039].
- [106] G. Das, M. C. Kumar and K. Samanta, Resummed inclusive cross-section in Randall-Sundrum model at NNLO+NNLL, JHEP 07 (2020) 040 [2004.03938].
- [107] J. M. Henn, M. Stahlhofen, M. Steinhauser and M. Wormser, Matter dependence of the four-loop QCD cusp anomalous dimension: from small angles to all angles, JHEP 04 (2020) 003 [1911.10174].
- [108] T. Huber, T. Hurth, E. Lunghi and J. Virto, Logarithmically Enhanced Contributions to the Angular Observables in $B \to V\ell\ell$, JHEP 08 (2019) 152 [1905.00965].
- [109] A. von Manteuffel, R. M. Schabinger and H. X. Zhu, The two-loop soft function for heavy quark pair production at future linear colliders, JHEP 08 (2020) 068 [2003.01798].